

Impingement Characteristics Investigation of Supercooled Large Droplets Based on Eulerian Method

YE Zekun¹, SHEN Xiaobin^{1*}, ZHAO Jingyu¹, LIN Guiping^{1,2}

1. Laboratory of Fundamental Science on Ergonomics and Environmental Control, School of Aeronautic Science and Engineering, Beihang University, Beijing 100191, P. R. China;

2. International Innovation Institute, Beihang University, Hangzhou 311115, P. R. China

(Received 15 February 2025; revised 20 March 2025; accepted 8 April 2025)

Abstract: This numerical simulation investigates the two-phase flow under the condition of supercooled large droplets impinging on the aircraft surface. Based on Eulerian framework, a method for calculating supercooled water droplet impingement characteristics is established. Then, considering the deformation and breaking effects during the movement, this method is extended to calculate the impingement characteristics of supercooled large droplets, as well as the bouncing and splashing effects during impingement. The impingement characteristics of supercooled large droplets is then investigated by this method. The results demonstrate that the deformation and breaking effects of supercooled large droplets have negligible influence on the impingement characteristics under the experimental conditions of this paper. In addition, the results of the impingement range and collection efficiency decrease when considering the bouncing and splashing effects. The bouncing effect mainly affects the mass loss near the impingement limits, while the splashing effect influences the result around the stagnation point. This investigation is beneficial for the analysis of aircraft icing and the design of anti-icing system with supercooled large droplet conditions.

Key words: aircraft icing; droplet impingement characteristics; supercooled large droplet (SLD); Eulerian method; numerical simulation

CLC number: V244.1

Document code: A

Article ID: 1005-1120(2025)02-0191-10

0 Introduction

Aircraft icing is one of the most important factors threatening the flight safety^[1]. The aircraft icing phenomenon is generated by supercooled water droplet impinging on the windward surface of the aircraft. Usually, the diameter of supercooled water droplet is less than 50 μm . In the air flow, only a small part of supercooled water droplets impinge around the stagnation point and freeze, while the others usually separate from the airfoil. On the other hand, supercooled large droplets (SLDs) are commonly defined as the water droplets with diameters larger than 50 μm , even reaching 1 000 μm in cloud^[2]. Due to the large diameter of SLD, its movement and impingement characteristics are dif-

ferent from that of conventional droplets. SLD are more likely to impinge on the windward surface with larger impingement range. The icing range may extend to the area which is not protected by anti-icing systems and flight accidents.

In 1994, an ATR-72 aircraft operated by American Eagle Airline experienced a fatal aircraft icing accident due to SLD. The aircraft went out of control and crashed, with 68 lives lost^[3]. Subsequently, researchers began to investigate the safety effects of SLD. During the movement of SLD, deformation and breakup phenomena may occur. When SLD impinge on the surface, their splashing and bouncing effects need to be considered. The splashed or rebounded droplets may reimpinge on

*Corresponding author, E-mail address: shenxiaobin@buaa.edu.cn.

How to cite this article: YE Zekun, SHEN Xiaobin, ZHAO Jingyu, et al. Impingement characteristics investigation of supercooled large droplets based on Eulerian method[J]. Transactions of Nanjing University of Aeronautics and Astronautics, 2025, 42(2): 191-200.

<http://dx.doi.org/10.16356/j.1005-1120.2025.02.004>

the downstream surface under the effect of air-flow^[4]. The characteristics of SLD affect the collection efficiency calculation during the movement and impingement processes, which influences the ice shape prediction of the aircraft surface further. Generally, the SLD motion characteristic is carried out by experiments. Researchers synthesize the criteria of droplet deformation and other phenomena through extensive experiments as well as obtained empirical or semiempirical correlation formulas^[5-7]. Researchers integrate the correlation formulas into the droplet impingement and icing models. Then they investigate SLD characteristics by comparing the simulation and experimental results, as well as refine the droplet impingement models^[8-10]. However, SLD calculation models and correlation formulas have particular range of applications. For each specific environmental condition, accurate results can only be obtained by selecting the proper correlations.

After about 30 years of research, a deeper understanding of SLD movement and icing characteristics has been achieved. Software such as LEWICE^[11] and FENSAP-ICE^[12] in computational fluid dynamics (CFD) has integrated relative functions for SLD. Relevant SLD environment and clause are added into the airworthiness management system, providing further guidance on the flight safety. However, owing to complexity of the movement and impingement process, current research about SLD remains limited. The goal of this paper is to extend an Eulerian method to investigate SLD effects, which considers the drag difference caused by SLD deformation, the breaking effects during movement, as well as the splashing and bouncing effects of impingement on surfaces. Then, simulations are performed to investigate the SLD effects, including deformation and break up during movement, as well as splashing and bouncing effects of impingement. The working mechanism of SLD effects on SLD impingement characteristics is analyzed. Finally, applicable ranges for models considering SLD effects are concluded from the results.

1 Mathematical Model

1.1 Droplet motion in Eulerian method

Eulerian method is widely used to investigate the droplet impingement characteristics. In Eulerian method, droplets are continuous and droplet volume fraction is introduced to define the ratio of droplet volume to the total air-droplet volume. Besides, Eulerian method is suitable for calculating the water collection efficiency on three-dimensional complex surfaces. In this work, an Eulerian method is used to establish the motion equations of conventional droplets. Then, the method is extended to include SLD effects. The deformation and break up of droplets are determined by Weber number. The splashing and bouncing models are established and solved, in which the deformation effect is considered but the break up effect is ignored.

Following assumptions for the motion and impingement of conventional droplets are provided: (1) Droplets are spherical with no deformation or breaking; (2) droplets do not collide or coalesce with each other, and there is no splashing or bouncing phenomena after impinging on the surface; (3) viscosity and pressure terms are not considered in the momentum equation of droplets; (4) there is no mass and heat transfer between the droplets and the surrounding air; (5) the turbulent effects on water droplets are neglected; (6) aerodynamic drag is considered as the only force acting on droplets and gravity and all unsteady forces are neglected; (7) drag acting on the water droplet is steady force. According to above assumptions, mass and momentum conservation equations of the droplet phase in the Eulerian method can be represented as^[13]

$$\frac{\partial}{\partial t}(\rho\alpha) + \nabla \cdot (\rho\alpha\mathbf{u}) = 0 \quad (1)$$

$$\frac{\partial}{\partial t}(\rho\alpha\mathbf{u}) + \nabla \cdot (\rho\alpha\mathbf{u} \otimes \mathbf{u}) = \rho\alpha K(\mathbf{u}_a - \mathbf{u}) \quad (2)$$

where \otimes is the vector product; α the droplet volume fraction; ρ the droplet density; \mathbf{u} the velocity of water droplets; \mathbf{u}_a the velocity of air; and K the air-droplet exchange coefficient, which is defined as

$$K = \frac{18\mu_a f}{\rho d_p^2} \quad (3)$$

where μ_a is the dynamic viscosity of the air, d_p the

diameter of the droplets, and f the drag function defined differently for different exchange-coefficient models. In Schiller and Naumann model, f is defined as^[14]

$$f = \frac{C_D Re}{24} \quad (4)$$

where C_D is the drag coefficient and is calculated as

$$C_D = \begin{cases} 24(1 + 0.15Re^{0.687})/Re & Re \leq 1000 \\ 0.44 & Re > 1000 \end{cases} \quad (5)$$

where Re is the relative Reynolds number, and is given as

$$Re = \frac{\rho_a |\mathbf{u}_a - \mathbf{u}| d_p}{\mu_a} \quad (6)$$

where ρ_a is the density of air.

By solving the airflow field and the droplet velocity field, the distribution of droplet volume fraction as well as the spatial field of droplet velocity can be obtained. Based on the above results, the local collection efficiency β on the surface can be calculated as

$$\beta = \frac{\alpha \mathbf{u} \cdot \mathbf{n}}{\alpha_\infty V_\infty} \quad (7)$$

where \mathbf{n} is the unit normal vector on the surface of control volume, V_∞ the freestream velocity, and α_∞ the droplet volume fraction in the freestream.

1.2 Deformation and breaking effects of SLD

Droplets with large diameter, influenced by air shear forces and surface tension during their movement, gradually transform from the sphere to the oblate disk. This shape change alters the drag force on droplets, then the drag coefficient in Eq.(5) is not applicable.

The Weber number We is usually used to evaluate the motion of SLD, defined as the ratio of droplet inertial force to the force of surface tension.

$$We = \frac{\rho_a d_p |\mathbf{u}_a - \mathbf{u}|^2}{\sigma_d} \quad (8)$$

where σ_d is the surface tension of the droplet.

Clift revises the drag coefficient formula of droplets during deformation according to the empirical formula about shape of the sphere and the oblate disk^[15]. A weighted value is used between the drag coefficient of the sphere ($C_{D, \text{sphere}}$) and the oblate disk ($C_{D, \text{disk}}$).

$$C_{D, \text{droplet}} = e C_{D, \text{disk}} + (1 - e) C_{D, \text{sphere}} \quad (9)$$

where $C_{D, \text{sphere}}$ can be obtained from Eq.(5), and

$C_{D, \text{disk}}$ and e are defined as

$$C_{D, \text{disk}} = \begin{cases} \frac{64(1 + 0.138Re^{0.792})}{\pi Re} & Re \leq 133 \\ 1.17 & Re > 133 \end{cases} \quad (10)$$

$$e = 1 - \frac{1}{(1 + 0.007\sqrt{We})^6} \quad (11)$$

When We of the droplet exceeds the critical value, the droplet will be unstable and break up into smaller water droplets. Hsiang et al.^[16] conducted research on the conditions for water droplet deformation, and the critical Weber number for droplets breaking is determined as 13. According to Ref. [16], when We is larger than 13, droplets will break up. The droplet velocity is assumed unchanged after breaking. The size of the droplets generated by breaking is calculated as

$$d_n = 6.2 \left(\frac{\rho_d}{\rho_a} \right)^{1/4} Re^{-0.5} d_o \quad (12)$$

where d_o is the initial droplet diameter.

1.3 Splashing and bouncing effects of SLD

When the supercooled water droplet impinges on the surface, it may generate various effects, including sticking, spreading, bouncing and splashing. It is considered that the whole mass of droplet remains on the surface when it is sticking and spreading. When the water droplet is considered bouncing, it indicates that the whole droplet has detached from the surface, and no mass remains on the surface. When splashing occurs, only portion of the droplet remains on the surface and participates in icing. In this paper, the splashing and bouncing models used in the LEWICE and FENSAP-ICE software are selected for investigation.

(1) LEWICE model

The mass loss of SLD splashing and bouncing effects is considered in the LEWICE model. It uses splash coefficient K as the criteria^[17].

$$K = \left(\frac{\rho_d^3 d_o^3 V_{d,n}^5}{\sigma_d^2 \mu_d} \right)^{1/4} \quad (13)$$

where $V_{d,n}$ is the normal component of the droplet velocity impinging on the surface. In addition, the threshold for splashing and bouncing phenomena is defined as

$$K_L = \frac{K_{Ln}}{(\sin \theta)^{1.25}} = \frac{\sqrt{K} f^{*-3/8}}{(\sin \theta)^{1.25}} > 200 \quad (14)$$

where θ is the tangential angle between the droplet velocity and the impingement surface, f^* the droplet frequency in dimensionless which is defined by liquid water content (LWC).

$$f^* = \frac{3}{2} \left(\frac{\text{LWC}}{\rho_d} \right)^{1/3} \quad (15)$$

A dimensionless mass loss coefficient (f_m) is defined to measure the mass loss caused by bouncing and splashing effects. The mass loss coefficient in LEWICE model is defined as

$$f_m = 0.7(1 - \sin \theta) [1 - e^{-0.0092(K_L - 200)}] \quad (16)$$

Finally, the local collection efficiency becomes

$$\beta_r = (1 - f_m) \beta \quad (17)$$

(2) FENSAP-ICE model

FENSAP-ICE offers users two approaches to handle SLD: by Post-Processing and by Body Force. Herein, the model used in the by Post-Processing approach is employed for analysis. The criterion proposed by Trujillo et al.^[18] is used to determine splashing

$$K_C > 540R^{-0.35} \quad (18)$$

where R is the constant of 0.005, K_C the Cossali number which is defined as

$$K_C = Oh^{-2/5} We_s \quad (19)$$

where Oh is the Ohnesorge number, and We_s the Weber number characterized by the normal component of the droplet velocity.

$$Oh = \frac{\mu_d}{\sqrt{\rho_d \sigma_d d_o}} \quad (20)$$

$$We_s = \frac{\rho_d d_o V_{d,n}^2}{\sigma_d} \quad (21)$$

Once the splashing phenomenon is determined by Eq.(18), then the droplet movement and the collection efficiency can be calculated according to modified model of Ref.[19]. The diameter of droplet after splashing (d_s) is given as below and it is constrained at $0.05 \leq d_s/d_o \leq 1$.

$$\frac{d_s}{d_o} = 8.72e^{-0.0281K_M} \quad (22)$$

The number of splash droplets (n_s) is constrained to a range of $n_s \leq 1000$ which is defined as

$$n_s = 1.676 \times 10^{-5} K_M^{2.539} \quad (23)$$

where the parameter K_M is defined as

$$K_M = Oh \cdot Re_s^{1.25} \quad (24)$$

where Re_s is the Reynolds number characterized by the normal component of the droplet velocity.

$$Re_s = \frac{\rho_d d_o V_{d,n}}{\mu_d} \quad (25)$$

Considering the mass loss coefficient of droplets splashing, the local collection efficiency β_s is shown as

$$\beta_s = \left(1 - \frac{m_s}{m_o}\right) \beta = \left(1 - n_s \left(\frac{d_s}{d_o}\right)^3\right) \beta \quad (26)$$

Bai et al.^[20] conducted investigations on the bouncing effect of the impingement model. It is provided that bouncing occurs when W_s is larger than 2 and less than 20. The local collection efficiency of the corresponding region of bouncing is zero.

2 SLD Effect Investigation

Herein, an Eulerian method is developed to obtain droplet impingement characteristics of SLD. Firstly, governing equations for the airflow field are solved with the help of FLUENT software. Then the Eulerian method with droplet deformation effect is solved with the help of the user-defined scalar (UDS) transport equations in FLUENT software, and the motion characteristics and the We distribution of water droplets are obtained. The specific solving process is in the references^[11,21-22]. After that, if the breaking effect of SLD is considered, the region where We is larger than 13, is marked and the droplet diameter in it is set to the value obtained in Eq.(12). Then the Eulerian equations are recalculated with the new droplet diameter distribution. With the distribution of droplet volume fraction and the spatial field of droplet velocity, the local collection efficiency β is obtained by Eq.(7) without the impingement effects of SLD. The mass loss coefficient can be calculated by different models under the splashing and bouncing effects, and the final distribution of the collection efficiency considering SLD effects can be obtained.

The MS(1)-317 airfoil with the chord length of 0.914 m is selected to analyze the SLD impingement characteristics. Based on our previous re-

search, the mesh that satisfied mesh independence was set up for the simulation^[23]. The structured mesh with a total of 25 200 was used, with refinement around the leading edge of the airfoil. Considering that the deformation and breaking of large water droplets have slight effect on the droplet collection efficiency as described in relative investigations^[24-25], the water droplets with a larger diameter (705 μm) are first selected for the calculation. The freestream velocity is 78.25 m/s, with the angle of attack (AOA) of -1.85° .

The distribution of We around the airfoil leading edge is shown in Fig.1. The Weber number is shown increase as the droplets getting closer to the stagnation point. The maximum value of the Weber number is about 72.2 and appears at the stagnation point. Since it exceeds the critical Weber number, the breaking phenomenon occurs. According to the airflow field and the spatial field of droplet velocity, changes of air velocity are sharply near the stagnation point. However, the inertia of the water droplet makes it move along the original direction. The velocity difference between the droplet and the air is large, so as the shear force of the water droplets. Hence, it increases We around this region, leading the droplets breaking.

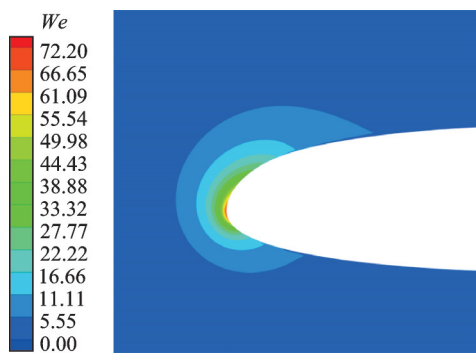


Fig.1 Weber number distribution contour around the leading edge

Fig.2 shows the influence of the deformation and breaking of SLD on the water collection efficiency, where the leading edge of the airfoil is represented by the curvilinear coordinate $s = 0$ and the top airfoil surface is represented by the positive value. Considering the droplet deformation effect only, the cal-

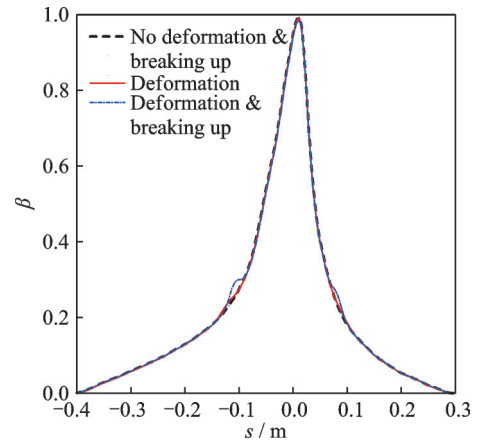


Fig.2 Comparison of collection efficiency on deformation and breaking effects of SLD

culatation result is consistent with the results of no SLD effects. It shows that the droplet deformation effect has little influence on the droplet impingement characteristics. According to the Ref.[25], when the droplet velocity and diameter are not very large, the deformation effect of SLD is small. Therefore, the present result is reasonable.

Considering both the deformation and breaking effects of SLD, the collection efficiency result is similar with the result without the SLD effect. A little difference can be seen between the two curves, which concentrates in the two certain regions. This is suggested to the droplet breaking around the stagnation point, and the smaller droplets would impinge on the downstream surface causing the mass increase. Although the breaking effects of SLD is small for the collection efficiency, the changes of SLD diameters would affect the splashing and bouncing processes^[24]. In addition, there would be multiple breaks of water droplets when the droplet velocity and the diameter are large, and the composite effects are very complex. Therefore, in this paper, the droplet breaking is not considered in the investigation of SLD splashing and bouncing effects.

Fig.3 shows the droplet collection efficiency curves considering splashing and bouncing effects with the LEWICE and FENSAP-ICE models, respectively. There is significant mass loss in most regions on the curve of LEWICE model, especially near the impingement limits. But there is almost no mass loss near the stagnation point. This is because

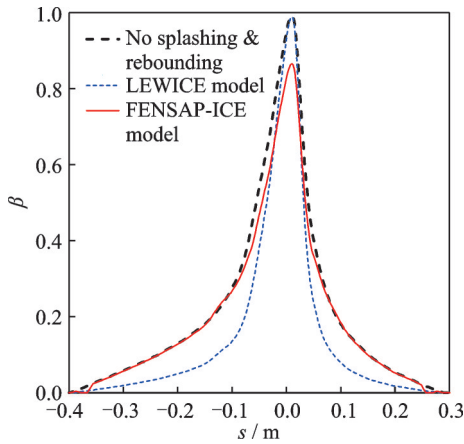


Fig.3 Comparison of collection efficiency on splashing and bouncing effects of SLD

the characterization of impingement angle in Eq.(16) in the LEWICE model. The droplet velocity is nearly perpendicular to the surface when it impinges on the surface near the stagnation point. Hence, the mass loss coefficient almost decreases to zero. Likewise, the mass loss coefficient is almost 1 when the droplet velocity is parallel to the surface. In contrast, there is large mass loss calculated by the FENSAP-ICE model near the stagnation point, which is caused by the splashing effect of SLD (Eq. (26)). The droplet collection efficiency near the impingement limit decreases to zero, which is attributed to the rebound of droplets impinging here. However, in the specific region (away from the stagnation point and the impingement limit regions), the mass loss of droplets is small. Because the splashing and bouncing models are not operative in this region.

3 Model Validation and Analysis

To evaluate the performance of the LEWICE model and FENSAP-ICE model, the simulation results are compared with the experimental results^[26]. Details of the calculation conditions are given in Table 1. Although the AOA is 0° in the experiment, a specific AOA of -1.85° is used on the free stream to match the experimental pressure distributions in the numerical simulations. As it is illustrated in Table 1, the median volumetric diameter (MVD) of SLD are $79 \mu\text{m}$, $137 \mu\text{m}$ and $168 \mu\text{m}$, respectively. In the simulation calculations, the diameters of

SLD are considered as the distribution within a specific range. The detailed droplet distributions are shown in Table 2, which is to match the experimental conditions. The local collection efficiency of SLD is obtained by solving the impingement results for each size and then weighting the results. Fig.4 shows the local collection efficiency distribution for each droplet size as well as the final weighted result of SLD with the median volumetric diameter of $137 \mu\text{m}$.

Table 1 Experimental conditions

Case	MVD/ μm	LWC/ $(\text{g}\cdot\text{m}^{-3})$	V_∞ / $(\text{m}\cdot\text{s}^{-1})$	AOA/ $(^\circ)$	T_∞ /K
1	79	0.496	78.25	0	280.9
2	137	0.68	78.25	0	280.9
3	168	0.747	78.25	0	280.9

Table 2 Droplet distributions

Case	Number-weighted/ %	Median volumetric diameter		
		79/ μm	137/ μm	168/ μm
1	5	9.136 017	13.326 21	15.087 4
2	10	22.392 15	41.755 55	52.538 82
3	20	39.928 43	81.439 27	102.252 5
4	30	77.472 93	138.227 4	172.097 2
5	20	123.594 3	206.798 4	264.377 8
6	10	166.606 1	285.250 6	395.583 2
7	3	206.474 9	382.611 1	530.898 7
8	1	241.536 7	471.470 4	624.474 1
9	0.5	270.438 9	534.098 4	705.360 5
10	0.5	310.314 7	693.944 5	1 110.787

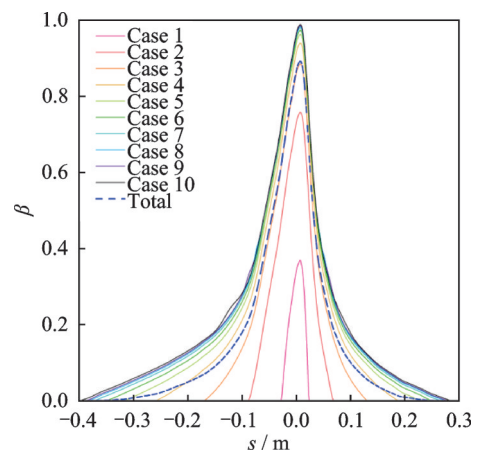


Fig.4 Local collection efficiency for each case with MVD of $137 \mu\text{m}$

Calculation results with only the bouncing effect of SLD are compared with experimental results

for different MVDs, as shown in Figs.5—7. As can be seen from the results, the bouncing of droplets occurs near the impingement limits. Results of FENSAP-ICE model show negligible differences compared to the model without considering the

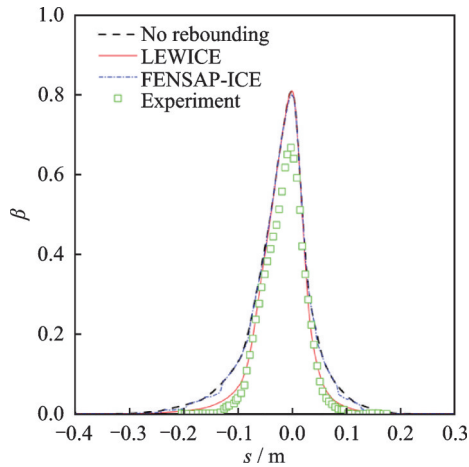


Fig.5 Comparison of collection efficiency on bouncing effect with MVD of $79 \mu\text{m}$

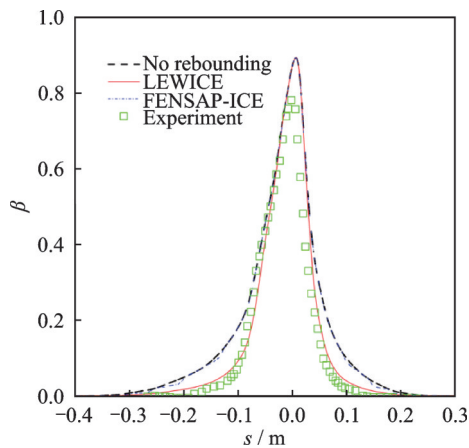


Fig.6 Comparison of collection efficiency on bouncing effect with MVD of $137 \mu\text{m}$

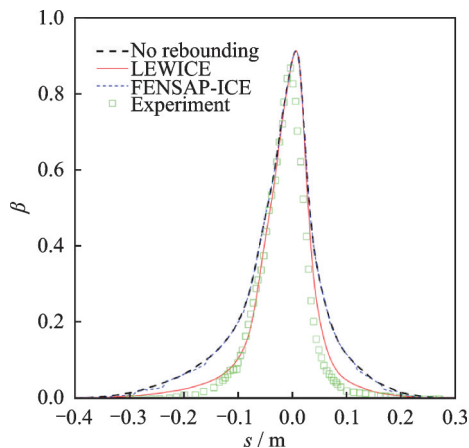


Fig.7 Comparison of collection efficiency on bouncing effect with MVD of $168 \mu\text{m}$

bouncing effect. On the other hand, LEWICE model has more mass loss around the impingement limits, which makes the collection efficiency more agreement with experimental results. This suggests that LEWICE model is more suitable to describe SLD bouncing effect.

Since the bouncing and splashing effects are both described in Eq.(17) in the LEWICE model, the droplet mass loss near the stagnation point is small, and the collection efficiency is different from the experimental data, indicating that the LEWICE model is not applicable to splashing effects. Therefore, the LEWICE model is used to investigate the bouncing effect of SLD and FENSAP-ICE model is used to evaluate SLD splashing effect. The calculation results are illustrated in Figs.8—10. It can be seen that the calculated results are in coincidence with the experimental results both at the stagnation point and the impingement limit. The results of the

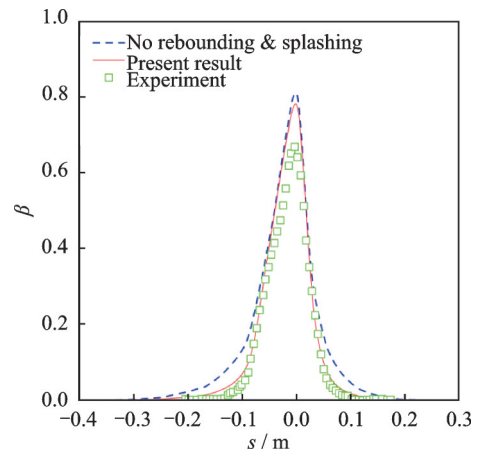


Fig.8 Comparison of collection efficiency on bouncing and splashing effects with MVD of $79 \mu\text{m}$

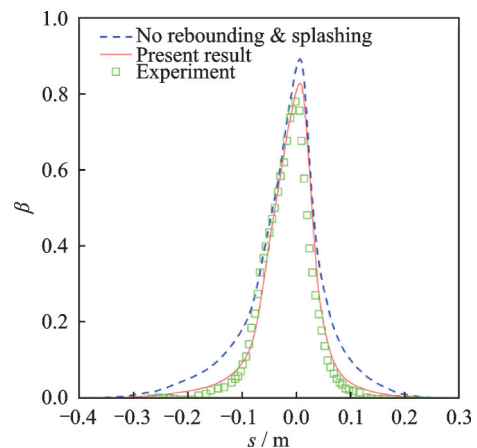


Fig.9 Comparison of collection efficiency on bouncing and splashing effects with MVD of $137 \mu\text{m}$

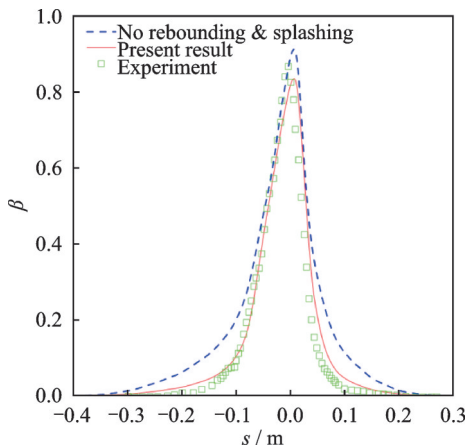


Fig.10 Comparison of collection efficiency on bouncing and splashing effects with MVD of $168 \mu\text{m}$

stagnation point are slightly larger than the experimental results with MVDs of $79 \mu\text{m}$ and $137 \mu\text{m}$, and slightly smaller with MVD of $168 \mu\text{m}$. It can be concluded that the combination of the LEWICE model and FENSAP-ICE model is suitable to describe splashing and bouncing effects of SLD, and performs well at certain MVDs.

To summarize, when the bouncing and splashing effects are integrated into the model, both the impingement range and collection efficiency decrease. The bouncing effect mainly influences the mass loss coefficient around the impingement limit and the splashing affects the results near the stagnation point. LEWICE model is effective for calculation of bouncing effect, which performs better for droplets in larger diameter. The bouncing results calculated by the FENSAP-ICE model are not very well, but its calculation of splashing effect can achieve good results when the droplet diameter is not too large. Combination of these two models would be an effective approach to describe the total SLD effects.

4 Conclusions

The Eulerian method is established and investigated for the SLD effects, which include the deformation and breaking effects as well as the bouncing and splashing effects. The deformation and breaking of water droplets movement and the bouncing and splashing effects of impingement process are numerically simulated, and the impingement characteris-

tics of SLD are obtained by different models. Based on the calculation results, the main conclusions are as follows: (1) The deformation and breaking effects of SLD have negligible influence on the droplet impingement characteristics in the present conditions. (2) When considering the bouncing and splashing effects of SLD, results of the impingement range and collection efficiency will be smaller than before. The bouncing effect mainly affects the mass loss calculation around the impingement limits, while the splashing effect influences the results near the stagnation point. (3) According to the comparison between calculation and experiment results, different bouncing and splashing models have their proper applying range. LEWICE model is effective for the calculation of bouncing effect, while calculation results of splashing effect performs better in FENSAP-ICE model. The combination model presented in this paper achieves satisfactory simulation results. With the investigation of SLD impingement characteristics, accuracy of ice shape prediction can be improved. It is also beneficial for the design of anti-icing systems, including the distribution of anti-icing surface and adjustment of heating power.

Reference

- [1] YAMAZAKI M, JEMCOV A, SAKAUE H. A review on the current status of icing physics and mitigation in aviation[J]. *Aerospace*, 2021, 8(7): 188.
- [2] CAO Y, XIN M. Numerical simulation of SLD icing phenomenon: A review[J]. *Archives of Computational Methods in Engineering*, 2020, 27(4): 1231-1265.
- [3] National Transportation Safety Board. In-flight icing encounter and loss of control: AAR—96-01[R]. [S.l.]: Transportation Research Board, 1996.
- [4] TAN S C, PAPADAKIS M. General effects of large droplet dynamics on ice accretion modeling[C]//Proceedings of the 41st Aerospace Sciences Meeting and Exhibit. Nevada, USA: AIAA, 2003.
- [5] ZHANG C, LIU H. Effect of drop size on the impact thermodynamics for supercooled large droplet in aircraft icing[J]. *Physics of Fluids*, 2016, 28(6): 062107.
- [6] HAN Z R, SI J T, WU D W. Contrast icing wind tunnel tests between normal droplets and supercooled large droplets[J]. *Aerospace*, 2022, 9(12): 844.
- [7] SHEN X B, ZHAO W Z, QI Z C, et al. Analysis of numerical methods for droplet impingement character-

- istics under aircraft icing conditions[J]. *Aerospace*, 2022, 9(8): 416.
- [8] IULIANO E, MINGIONE G, PETROSINO F, et al. Eulerian modeling of SLD physics towards more realistic aircraft icing simulation[C]//Proceedings of the AIAA Atmospheric and Space Environments Conference. Toronto, Canada: AIAA, 2010.
- [9] PRINCE RAJ L, ESMAELIFAR E, JEONG H, et al. Computational simulation of glaze ice accretion on a rotorcraft engine intake in large supercooled droplet icing conditions[C]//Proceedings of the AIAA SCITECH 2022 Forum. San Diego, USA: AIAA, 2022.
- [10] BROEREN A P, LEE S, TSAO J. Large-drop ice accretion test results for a large scale swept wing section[C]//Proceedings of the AIAA Icing Characteristics on Large Scale Swept Wing. Ohio, USA: [s.n.], 2021.
- [11] WRIGHT W B. Further refinement of the LEWICE SLD model[C]//Proceedings of the 44th AIAA Aerospace Sciences Meeting and Exhibit. Nevada, USA: AIAA, 2006.
- [12] HONSEK R, HABASHI W G, AUBÉ M S. Eulerian modeling of in-flight icing due to supercooled large droplets[J]. *Journal of Aircraft*, 2008, 45(4): 1290-1296.
- [13] SHEN X B, XIAO C H, NING Y J, et al. Research on the methods for obtaining droplet impingement characteristics in the Lagrangian framework[J]. *Aerospace*, 2024, 11(3): 172.
- [14] Ansys Inc. Ansys fluent 19.0 UDF manual[M]. New Hampshire: Ansys Inc, 2019.
- [15] CLIFT R, GRACE J R, WEBER M E. Bubbles, drops and particles[M]. New York: Academic Press, 1978.
- [16] HSIANG L P, FAETH G M. Second drop breakup in the deformation regime[C]//Proceedings of the 30th Aerospace Sciences Meeting and Exhibit. [S.l.]: AIAA, 1992.
- [17] WILLIAM B W, MARK G P. Semi-empirical modeling of SLD physics[C]//Proceedings of the Aerospace Sciences Meeting and Exhibit. [S.l.]: National Aeronautics and Space Administration, 2004.
- [18] TRUJILLO M F, MATHEWS W S, LEE C F, et al. Modelling and experiment of impingement and atomization of a liquid spray on a wall[J]. *International Journal of Engine Research*, 2000, 1(1): 87-105.
- [19] MUNDO C, TROPEA C, SOMMEFELD M. Numerical and experimental investigation of spray characteristics in the vicinity of a rigid wall[J]. *Experimental Thermal and Fluid Science*, 1997, 15(3): 228-237.
- [20] BAI C, GOSMAN A D. Development of methodology for spray impingement simulation[J]. *Sae Transactions*, 1995. DOI: 10.4271/950283.
- [21] DU Chenhui, YU Jia, LIN Guiping, et al. Analysis on supercooled large droplet impingement characteristics and ice shape of two-dimensional airfoils[J]. *Journal of Aerospace Power*, 2014, 29(4): 783-791. (in Chinese)
- [22] YANG S, LIN G, SHEN X. An Eulerian method for water droplet impingement prediction and its implementations[C]//Proceedings of the 1st International Symposium on Aircraft Airworthiness. Beijing, China: [s.n.], 2009.
- [23] ZHAO W, NING Y, WU Y, et al. Mesh impact analysis of Eulerian method for droplet impingement characteristics under aircraft icing conditions[J]. *Transactions of Nanjing University of Aeronautics and Astronautics*, 2023, 40(2): 148-158.
- [24] BAE J, YEE K. Numerical investigation of droplet breakup effects on droplet-wall interactions under SLD conditions[J]. *International Journal of Aeronautical and Space Sciences*, 2021, 22(5): 1005-1018.
- [25] SUTHYVANN M, ADELAIIDA G M. Influence of the deformation in the collection efficiency on a profile applying DRD model[C]//Proceedings of Numerical Models for Ice Accretion Simulation Part 2. [S.l.]: [s.n.], 2021.
- [26] PAPADAKIS M, WONG S, RACHMAB A A, et al. Large and small droplet impingement data on airfoils and two simulated ice shapes: NASA/TM—2007-213959[R]. Ohio, USA: NASA Glenn Research Center, 2007.

Acknowledgements This work was supported in part by the National Natural Science Foundation of China (No. 51806008), the Open Fund of Key Laboratory of Rotor Aerodynamics Key Laboratory (No.RAL202104-2).

Authors

The first author Mr. YE Zekun received the B.S. degree in aerospace engineering from School of General Engineering, Beihang University, Beijing, China, in 2024. He is preparing for the M.S. degree in the same school. His research has focused on numerical simulation of energy management of aircraft icing and de-icing.

The corresponding author Dr. SHEN Xiaobin received the Ph.D. degree in ergonomics and environmental control from Beihang University, Beijing, China, in 2013. His research includes aircraft icing/anti-icing technology, heat transfer simulation in complex environments, aircraft environmental control, and energy management.

Author contributions Mr. YE Zekun designed the study,

wrote the manuscript and designed the article structure. Dr. SHEN Xiaobin guided the method and modified the model. Ms. ZHAO Jingyu conducted analysis and the numerical simulation. Prof. LIN Guiping contributed to the design and

discussion of the study. All authors commented on the manuscript draft and approved the submission.

Competing interests The authors declare no competing interests.

(Production Editors: XU Chengting, WANG Jie)

基于欧拉法的过冷大水滴撞击特性研究

叶泽坤¹, 申晓斌¹, 赵静宇¹, 林贵平^{1,2}

(1. 北京航空航天大学航空科学与工程学院人机工效与环境控制重点学科实验室, 北京 100191, 中国;

2. 北京航空航天大学国际创新研究院, 杭州 311115, 中国)

摘要: 针对过冷大水滴条件下的飞机表面结冰威胁, 开展空气-大水滴两相流动数值仿真研究。首先基于欧拉法建立了普通尺寸过冷水滴的运动撞击特性计算方法; 然后考虑过冷大水滴运动过程中的变形与破碎及撞击时的反弹与飞溅现象, 将该方法扩展到过冷大水滴的撞击特性计算中; 最后用扩展后的方法, 计算分析过冷大水滴的运动撞击特性。结果表明, 过冷大水滴的变形与破碎效应在本文实验条件下对水滴撞击特性的影响较小; 考虑当大水滴反弹与飞溅时, 计算的撞击范围和收集系数都变小; 反弹效应主要影响撞击极限附近的质量损失, 飞溅效应则决定驻点附近的结果。本文的研究对过冷大水滴条件下的飞机结冰分析与防除冰系统设计优化具有指导意义。

关键词: 飞机结冰; 水滴撞击特性; 过冷大水滴; 欧拉法; 数值仿真